JOURNAL OF BACTERIOLOGY, Oct. 2006, p. 7123–7131 Vol. 188, No. 20
0021-9193/06/$08.00+0 doi:10.1128/JB.00757-06

Molecular and Biochemical Characterization of α-Glucosidase and α-Mannosidase and Their Clustered Genes from the Thermoacidophilic Archaeon *Picrophilus torridus*†

Angel Angelov,[1] Mateusz Putyrski,[1,2] and Wolfgang Liebl[1]*

Institute of Microbiology and Genetics, University of Goettingen, Grisebachstrasse 8, D-37077 Goettingen, Germany,[1] and Institute of Microbiology, Department of Bacterial Genetics, Warsaw University, Miecznikowa 1, 02-096 Warsaw, Poland[2]

Received 26 May 2006/Accepted 30 July 2006

The genes encoding a putative α-glucosidase (*aglA*) and an α-mannosidase (*manA*) appear to be physically clustered in the genome of the extreme acidophile *Picrophilus torridus*, a situation not found previously in any other organism possessing *aglA* or *manA* homologs. While archaeal α-glucosidases have been described, no α-mannosidase enzymes from the archaeal kingdom have been reported previously. Transcription start site mapping and Northern blot analysis revealed that despite their colinear orientation and the small intergenic space, the genes are independently transcribed, both producing leaderless mRNA. *aglA* and *manA* were cloned and overexpressed in *Escherichia coli*, and the purified recombinant enzymes were characterized with respect to their physicochemical and biochemical properties. AglA displayed strict substrate specificity and hydrolyzed maltose, as well as longer α-1,4-linked maltooligosaccharides. ManA, on the other hand, hydrolyzed all possible linkage types of α-glycosidically linked mannose disaccharides and was able to hydrolyze α3,α6-mannopentaose, which represents the core structure of many triantennary N-linked carbohydrates in glycoproteins. The probable physiological role of the two enzymes in the utilization of exogenous glycoproteins and/or in the turnover of the organism's own glycoproteins is discussed.

Picrophilus torridus is an extremophilic organism belonging to the euryarchaeal phylum in which there has been considerable interest in the last few years due to its astonishing ability to live under highly acidic conditions, at pH values close to and even below pH 0. Strains of this species were first isolated from a dry solfataric field in northern Japan (28). In such geothermally heated habitats, the acidity is due to the sulfuric acid formed by the oxidation of volcanic sulfur to SO_3, which reacts with water to produce H_2SO_4, and the acid concentration can be further increased by water evaporation. *P. torridus* grows optimally at 60°C and pH 0.7 and requires oxygen and complex organic compounds. The specialization of *Picrophilus* strains for growth in extremely acidic habitats is evident from their inability to grow at pH values above 4.0 and their unusually low intracellular pH (pH 4.6), which distinguishes them from other thermoacidophilic organisms, which maintain internal pH values close to neutral (35, 39). The complete genome sequence of *P. torridus* has been reported previously (11), and it provides a basis for obtaining a better understanding of the mechanisms that enable survival under such extreme acid conditions.

α-Glucosidases are enzymes that typically catalyze the hydrolysis of terminal, nonreducing, 1,4-linked D-glucose residues. In contrast to glucoamylases (glucan 1,4-α-glucosidases), α-glucosidases favor oligosaccharides as substrates, while polysaccharides are hydrolyzed relatively slowly or not at all. Numerous α-glucosidases from bacteria and eukaryotes have been characterized, and the majority of them have been from mesophilic organisms. The previously reported archaeal representatives are the enzymes from *Sulfolobus solfataricus* (23), *Pyrococcus furiosus* (3), and *Thermococcus* sp. (21), and only the *S. solfataricus* α-glucosidase has been produced recombinantly (24).

Eukaryal α-mannosidases are membrane-bound or cytosolic proteins with important biological functions in glycoprotein processing and catabolism (5). In bacteria, a few enzymes with α-mannosidase activity have been described; examples include a secreted 1,2-α-mannosidase from *Bacillus* sp. (17), a cytoplasmic enzyme from *Mycobacterium tuberculosis* (22), and a thermoactive cytosolic α-mannosidase from *Thermotoga maritima* (18). An interesting bacterial representative of these enzymes has been found in *Escherichia coli*, and this enzyme is presumably involved in the utilization of the compatible solute 2-α-mannosyl-D-glycerate (27). Several archaeal sequences annotated as α-mannosidase can be found in the public databases; most of them originated from whole-genome sequencing projects. However, an archaeal α-mannosidase has not been characterized previously, and the physiological role of α-mannosidases in the domain *Archaea* remains obscure.

MATERIALS AND METHODS

Strains and growth conditions. *P. torridus* DSM 9790 was obtained from the Deutsche Sammlung von Mikroorganismen und Zellkulturen and was grown aerobically at 60°C and pH 0.7 in Brock's medium supplemented with 0.2% (vol/vol) yeast extract, as described by Schleper et al. (28). This medium contained (per liter) 1.32 g $(NH_4)_2SO_4$, 0.28 g KH_2PO_4, 0.25 g $MgSO_4 \cdot 7H_2O$, 0.07 g $CaCl_2 \cdot 2H_2O$, 0.02 g $FeCl_3 \cdot 6H_2O$, 1.8 mg $MnCl_2 \cdot 4H_2O$, 4.5 mg $Na_2B_4O_7 \cdot 10H_2O$, 0.22 mg $ZnSO_4 \cdot 7H_2O$, 0.05 mg $CuCl_2 \cdot 2H_2O$, 0.03 mg $Na_2MoO_4 \cdot 2H_2O$, 0.03 mg $VOSO_4 \cdot 2H_2O$, and 0.01 mg $CoSO_4$. The pH was adjusted with concentrated H_2SO_4.

E. coli XL1-Blue was used as a general host for DNA manipulations. For

* Corresponding author. Mailing address: Institut für Mikrobiologie und Genetik, Georg-August-Universität Göttingen, Grisebachstr. 8, D-37077 Göttingen, Germany. Phone: 49-551-393795. Fax: 49-551-393793. E-mail: wliebl@gwdg.de.

† Supplemental material for this article may be found at http://jb.asm.org/.

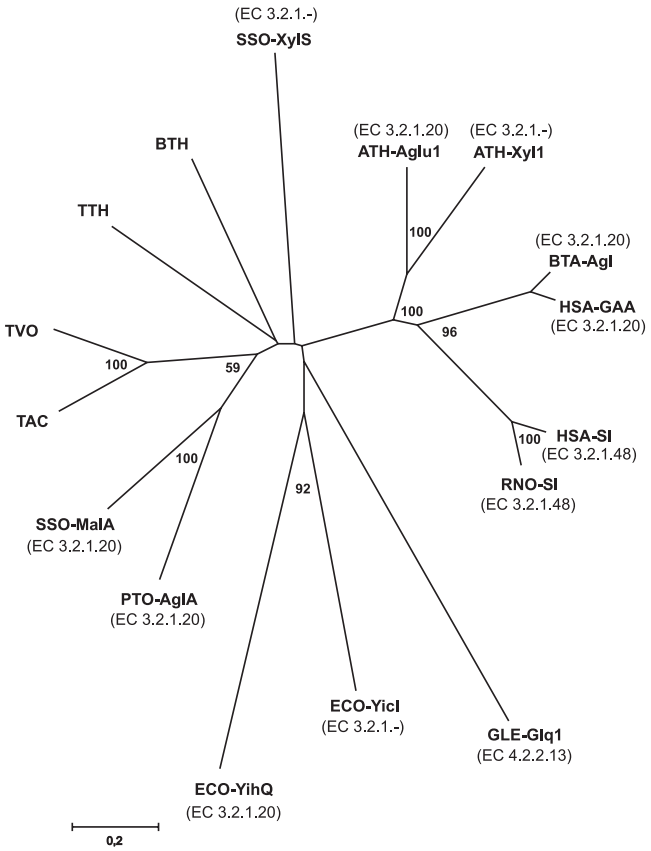

FIG. 1. Phylogenetic tree of selected members of glycoside hydrolase family 31. The EC numbers for protein sequences with known substrate specificities are given in parentheses; the numbers at the nodes are bootstrap confidence values. The following abbreviations are used (accession numbers are in parentheses): PTO-AglA, *P. torridus* AglA (AAT42677); SSO-MalA, *S. solfataricus* MalA (AAK43151); SSO-XylS, *S. solfataricus* XylS (AAK43123); TAC, *T. acidophilum* (CAC11443); TVO, *T. volcanium* (BAB60467); BTH, *B. thermoamyloliquefaciens* (BAA76396); TTH, *T. thermophilus* (AAS82549); ATH-Aglu1, *Arabidopsis* thaliana Aglu1 (AAB82656); ATH-Xyl1, *A. thaliana* Xyl1 (AAD05539); HSA-GAA, *Homo sapiens* GAA (CAA68763); HSA-SI, *H. sapiens* SI (CAA45140); BTA-Agl, *Bos taurus* Agl (AAF81637); RNO-SI, *Rattus norvegicus* SI (AAA65097); GLE-Glq1, *Gracilariopsis lemaneiformis* Glq1 (CAB51910); ECO-YihQ, *E. coli* YihQ (AAB03011); ECO-YicI, *E. coli* YicI (AAA62009).

expression of the recombinant AglA and ManA enzymes, an *E. coli* strain was constructed by introducing the 4.7-kb plasmid conferring streptomycin resistance [obtained from *E. coli* BL21-CodonPlus(DE3)-RIPL (Stratagene)] into *E. coli* BL21 (Novagen) to obtain *E. coli* BL21RS. This strain was transformed with each of five chaperone-encoding plasmids (TAKARA BIO). The resulting strains were cultivated in Luria-Bertani medium at 37°C, and when necessary, 50 μg/ml ampicillin and/or 34 μg/ml chloramphenicol, 25 μg/ml kanamycin, and 50 μg/ml streptomycin were added to the medium to maintain the plasmids.

Sequence and phylogenetic analyses. The sequences of glycoside hydrolase family 31 (GHF 31) members used for phylogenetic tree construction (Fig. 1) were selected based on the available biochemical data (substrate specificity), with the exception of the enzymes from *Thermoplasma acidophilum*, *Thermoplasma volcanium*, *Thermoplasma thermophilus*, and *Bacillus thermoamyloliquefaciens*. Multiple-sequence alignments were constructed using the program ClustalW v1.83 (available at http://www.ebi.ac.uk/clustalw/) with default parameters. The phylogenetic tree in Fig. 1 was constructed using the Mega2 program (15) and distance neighbor joining based on pairwise distances between amino acid sequences and global gap removal. Confidence limits for branch points were estimated from 1,000 bootstrap replications.

Cloning of the *P. torridus* α-glucosidase and α-mannosidase genes and expression in *E. coli*. The *P. torridus* open reading frames (ORFs) PTO0091 and PTO0092 encode putative α-mannosidase and α-glucosidase and were designated *manA* and *aglA*, respectively (11). Cloning of the *P. torridus* ORF PTO0092 was accomplished by amplifying the genome region surrounding the *aglA* gene with primers 985reg_for (5′-TGCGGAATACCATTCGGCAGCAT-3′) and 985reg_rev (5′-TCAATACGGCCGCACCAACAAGT-3′) using genomic DNA as the template. The 2,996-bp product contained a 500-bp DNA sequence upstream of the gene's start codon (ATG) and a 500-bp sequence downstream of its stop codon (amber) and was cloned in pCR4-TOPO using a TOPO cloning kit (Invitrogen). The vector obtained (pCR-*aglA* reg) was cut with BspHI (NcoI compatible) and EagI (NotI compatible), and the fragment containing the *aglA* gene was ligated with pET24d (Novagen) digested with NcoI and NotI. For cloning of the *manA* gene, primers 984.F-nco (5′-CACCATGGTAAACATTA AAAGAAAGC-3′) and 984.R (5′-ATTCAGGTTTAACATTGGCATC-3′) were used to amplify the *P. torridus* ORF PTO0091 with genomic DNA as the template. The PCR product obtained was cloned into pDrive (QIAGEN PCR cloning kit), and the 3,084-bp NcoI-SacI fragment containing the *manA* gene (NcoI was introduced with the 984.F-nco primer; the restriction site is underlined) was cloned in pET24d digested with the same enzymes. The resulting recombinant plasmids, p24-*aglA* and p24-*manA*, were transformed in *E. coli* BL21RS, carrying each of five different plasmids for homologous chaperones (TAKARA BIO). Expression of the *aglA* gene in *E. coli* was induced by adding isopropyl-β-D-thiogalactopyranoside (IPTG) at a concentration of 0.1 mM after the cell culture optical density reached 0.5. The *manA* gene was expressed without addition of IPTG.

Purification of recombinant AglA and ManA and molecular weight determination. The recombinant AglA and ManA enzymes were purified from *E. coli* BL21RS grown in 2 liters of Luria-Bertani medium. The cells were harvested by centrifugation (15 min, 6,000 × *g*), washed with 50 mM Tris-HCl buffer (pH 8.0) for the ManA samples or with 50 mM acetate buffer (pH 5.0) for the AglA samples, and lysed by twofold passage through a French press. AglA was purified further by heat treatment (15 min at 67°C), by anion-exchange chromatography in 50 mM Tris-HCl (pH 8.0) on a Source Q30 column (Amersham Biosciences) using a linear NaCl gradient (0 to 1.0 M), and finally by gel filtration on a Superdex 200 column (Amersham Biosciences) in Tris-HCl (pH 8.0) containing 150 mM NaCl. For purification of ManA, 1 M $(NH_4)_2SO_4$ was added to the cell lysate before hydrophobic interaction chromatography on a HighLoad Phenyl Sepharose column (Amersham Biosciences), which was followed by anion-exchange (Source Q30) and gel filtration (Superdex 200) steps using the same conditions that were used for AglA. After each purification step the fractions obtained were evaluated for specific enzyme activity and subjected to sodium dodecyl sulfate (SDS)-polyacrylamide gel electrophoresis (PAGE), and the most active fractions were pooled, concentrated (Amicon Ultra columns; Millipore), and dialyzed against the corresponding buffer.

Gel filtration chromatography (Superdex 200 equilibrated with 50 mM Tris-HCl [pH 8.0]–150 mM NaCl) was used to determine the oligomerization state of the recombinant enzymes. The following proteins, purchased from Boehringer Mannheim, were used as standards: cytochrome *c* (12.5 kDa), bovine albumin (68 kDa), catalase (240 kDa), and ferritin (450 kDa).

Enzyme assays and kinetics. (i) Standard assay. In the standard assay, α-glucosidase and α-mannosidase activities were determined with *p*-nitrophenyl-α-D-glucopyranoside and *p*-nitrophenyl-α-D-mannopyranoside (pNP-Man), respectively, purchased from Sigma. The reaction mixtures (total volume, 50 μl) contained 50 mM acetate buffer (pH 5.0), 10 mM *p*-nitrophenyl substrate, and enzyme solutions. When α-mannosidase activity was assayed, the reaction buffer was supplemented with 1 mM $CdCl_2$. After a 10-min incubation at 85°C for AglA or at 70°C for ManA, the reactions were stopped by addition of 100 μl 1 M Na_2CO_3, and the absorbance at 420 nm was determined. Specific activity was expressed in μmol of *p*-nitrophenol released (molar absorption coefficient, $1.12 \times 10^4\ M^{-1}\ cm^{-1}$) per min per mg of protein under the conditions specified above.

(ii) Alternative assays. The activities of the two enzymes with natural substrates were analyzed by thin-layer chromatography (TLC) on silica gel plates (Silica Gel 60 F_{254}; Merck), using 1-propanol–water–ethyl acetate (6:3:1, vol/vol/vol) as the mobile phase. The reaction products were detected by spraying the chromatograms with aniline-diphenylamine reagent (1% [wt/vol] diphenylamine and 1% [vol/vol] aniline in acetone mixed with 0.1 volume of 87% [vol/vol] phosphoric acid prior to use) and baking them for 10 min at 160°C.

The α-glucosidase and α-mannosidase activities with natural substrates were measured quantitatively by determining the amounts of monosaccharides (glucose and mannose, respectively) released after enzyme treatment. The assays were performed like the standard assay but with longer incubation times (15

TABLE 1. Primers used in this study

Primer	Sequence (5′–3′)	Description
984.RC-rev1	TATAATGAGCCGGTGTCCTG	*manA* 5′-RACE inner
984.RC-rev2	CAGTGTCCAATTGCCAAGATG	*manA* 5′-RACE outer
985.RC-rev1	TTAAGGCCTATGTCGATCTC	*aglA* 5′-RACE inner
985.RC-rev2	TTGATATCTGGTGCCCGAGTG	*aglA* 5′-RACE outer
984.F	GGATTCCTGTAGGAGGTATG	*manA* quantitative RT-PCR forward
984.R	ATGAATCCGGTAGCCAAC	*manA* quantitative RT-PCR reverse
985.F	GGAGCGCACTTCACTACAC	*aglA* quantitative RT-PCR forward
985.R	GCCTCGTATGTTGCCTTAGC	*aglA* quantitative RT-PCR reverse

min), and the reactions were stopped by heating the samples at 100°C for 15 min. The amount of glucose formed was estimated with a glucose oxidase/peroxidase-coupled assay (Sigma procedure no. 510), and the mannose concentration was determined with a coupled assay utilizing the enzymes hexokinase (Roche), phosphomannose isomerase (Sigma), phosphoglucose isomerase (Sigma), and glucose-6-phosphate dehydrogenase (Sigma) essentially as described by Etchison and Freeze (10). The substrates tested with ManA were α-1,2-, α-1,3-, methyl-*O*-α-1,4-, and α-1,6-mannobiose and α-Man-(1→3)(α-Man-[1→6])-α-Man-(1→6)(α-Man-[1→3])-Man (referred to as α3,α6-mannopentaose below) (Sigma).

Transcription analysis. *P. torridus* RNA was prepared from 10 ml of a culture grown to the end of the exponential phase using either an RNeasy mini kit (QIAGEN) or the RNAgents total RNA isolation system (Promega) as described by the manufacturers. The cells (approximately 4×10^8 cells) were centrifuged ($6{,}000 \times g$), washed in 50 mM acetate buffer (pH 5.0), and lysed by resuspending them in 100 μl of 50 mM Tris-HCl (pH 8.0).

Northern blot analysis. For Northern blot preparation, total *P. torridus* RNA was separated on 1.2% agarose gels in the presence of 0.2 M formaldehyde in morpholinepropanesulfonic acid (MOPS) buffer, followed by capillary transfer to a Hybond XL membrane (Amersham Biosciences), as described by Sambrook et al. (26) except that hybridization was performed with UltraHyb buffer (Ambion) at 50°C. The radioactive DNA probe was generated by random primer synthesis with a HexaLabel DNA labeling kit (Fermentas) and α-^{32}P-labeled deoxynucleoside triphosphates using a 583-bp fragment of the *aglA* gene (PstI-HindIII fragment of pCR-*aglA* reg) as the template.

Mapping of *aglA* and *manA* transcription start sites. RNA ligase-mediated rapid amplification of cDNA ends (RLM-RACE) was used to determine the transcription start sites of the *aglA* and *manA* genes (FirstChoice RLM-RACE kit; Ambion), using the protocol of the manufacturer. Two independent replications of the 5′ RLM-RACE procedure were carried out, including a control without tobacco acid pyrophosphatase treatment. The cDNA obtained was subjected to nested PCR with SuperTaq Plus DNA polymerase (Ambion) using the primers listed in Table 1, and the PCR products were column purified (QIAquick PCR purification; QIAGEN) and cloned using a StrataClone PCR cloning kit (Stratagene). A total of 10 colonies per gene were analyzed, and the insert was sequenced in both directions (ABI 3700; Applied Biosystems).

Quantitative RT-PCR. The *aglA* and *manA* transcripts were quantified by reverse transcription (RT) with RevertAid Moloney murine leukemia virus reverse transcriptase (Fermentas), followed by absolute real-time PCR (for primer sequences see Table 1) using SYBR green (qPCR MasterMix Plus for SYBR green I with fluorescein; Eurogentec) with an iCycler (Bio-Rad). External standard curves were generated for both genes with recombinant RNAs (recRNAs) covering the range from 1×10^4 to 1×10^{10} molecules per RT reaction mixture. Recombinant RNAs were synthesized for both genes in in vitro T7 promoter-directed transcription reactions with linearized p24-*manA* and p24-*aglA* as the templates (T7 RNA polymerase; Fermentas). After purification by phenol-chloroform extraction, the recRNAs obtained were serially diluted in water, and 2 ng of a total *E. coli* RNA preparation was added to each tube in order to compensate for background effects and mimic a natural RNA distribution like that in native total RNA (20). The recRNA dilutions were subjected in duplicate to RT and quantitative PCR, and plots of cycle threshold versus log recRNA copy number were generated. The recRNA external standard curves showed PCR efficiencies of 108.8% ($R^2 = 0.978$) for the *manA* gene and 100.8% ($R^2 = 0.993$) for the *aglA* gene over the range tested. Quantification of the native *aglA* and *manA* transcripts was performed in duplicate for three dilutions of the total *P. torridus* RNA, and the intraassay and interassay coefficients of variation were estimated.

RESULTS

Phylogenetic analysis of *P. torridus* α-glucosidase and α-mannosidase. The *P. torridus* ORF PTO0092 translation product (AglA), annotated as α-glucosidase (EC 3.2.1.20), displayed a high level of amino acid sequence similarity (38.6% identity) to the previously characterized ortholog from *S. solfataricus*, MalA (9, 24). The 645-residue protein could be classified as a member of GHF 31 based on the presence of the conserved active site pattern [GF]-[LIVMF]-W-x-D-M-[NSA]-E characteristic of this family (Carbohydrate Active Enzymes database [http://www.cazy.org]) (4) (see Fig. 1S in the supplemental material). At present, this family contains numerous enzymes of organisms belonging to all major branches of the phylogenetic tree, including 10 enzymes of archaeal origin having several known activities, such as α-glucosidase (EC 3.2.1.20), sucrase-isomaltase (EC 3.2.1.48 and EC 3.2.1.10), α-xylosidase (EC 3.2.1.-), α-glucan lyase (EC 4.2.2.13), and isomaltosyltransferase (EC 2.4.1.-). Phylogenetic analysis of the AglA sequence performed by the neighbor-joining tree method (15) revealed that this sequence is more similar to orthologs from members of the genus *Sulfolobus* than to sequences from members of the phylogenetically closely related genus *Thermoplasma* (Fig. 1).

The *P. torridus* α-mannosidase gene (*manA*, ORF PTO0091) codes for a 952-amino-acid protein and is located immediately upstream of *aglA*. Analysis of the protein sequence indicated that ManA is a member of GHF 38, which contains enzymes with α-mannosidase activity (EC 3.2.1.24) (see Fig. S2 in the supplemental material). GHF 38 currently includes some archaeal representatives (6 enzymes), many bacterial representatives (75 enzymes), and many eukaryal representatives (76 enzymes). Extensive phylogenetic analyses have shown that the currently available α-mannosidase sequences form three distinct groups (7, 11). The archaeal representatives fall into clade III of the α-mannosidase phylogeny, which is the most ancient and taxonomically diverse group of α-mannosidases (12), and these representatives seem to be restricted to the orders *Sulfolobales* (*S. solfataricus* and *Sulfolobus tokodaii*), *Thermoplasmatales* (*P. torridus* and *T. volcanium*), and *Thermococcales* (*Pyrococcus horikoshii*). Interestingly, BLAST analysis revealed that the ManA protein and its homologs from *T. volcanium* and *S. tokodaii* contain a distinct N-terminal domain which is not found in the rest of the available α-mannosidase sequences. So far, no archaeal α-mannosidase enzyme has been characterized.

Both AglA and ManA lacked detectable signal peptide se-

TABLE 2. Purification of AglA and ManA

Enzyme	Step	Total protein (mg)	Total activity (U)	Sp act ($U \cdot mg^{-1}$)	Yield (%)	Purification (fold)
AglA	Cell extract	171.3	151.7	0.88	100	1
	Heat treatment	35.1	95.1	2.71	62.7	3.1
	Source Q	1.01	22.7	22.52	14.9	25.6
	Superdex 200	0.41	14.2	34.56	9.4	39.3
ManA	Cell extract	2,166	541.5	0.25	100	1
	Phenyl Sepharose	380	190	0.50	35.1	2
	Source Q	1.92	38.6	20.1	7.2	80.5
	Superdex 200	0.13	7.7	59.2	1.4	237.5

quences (SignalP 3.0) (1). Also, the native α-glucosidase and α-mannosidase activities measured in fractionated *P. torridus* cell extracts were associated with the soluble fraction (not shown), suggesting that the two enzymes are located in the *P. torridus* cytosol.

Purification of recombinant *P. torridus* α-glucosidase and α-mannosidase, enzyme properties, and substrate specificity. Both enzymes were found to be expressed in the active form in *E. coli* only after the host was cotransformed with plasmids containing the genes for host chaperones and for tRNAs for codons which are rare in *E. coli*. Therefore, *E. coli* BL21 derivatives were constructed that harbored a plasmid for rare *E. coli* tRNAs (*E. coli* BL21RS) (see Materials and Methods) and each of five different plasmids encoding *E. coli* chaperones. The highest activities were observed after coexpression of the *P. torridus* α-mannosidase gene (*manA*) with *groES-groEL* and after coexpression of the α-glucosidase gene (*aglA*) with *groEL-groES-tig* (data not shown). These cells were used for overexpression and purification of the recombinant enzymes. Both enzymes were purified to electrophoretic homogeneity by use of heat treatment (for AglA), followed by hydrophobic interaction, anion-exchange, and size exclusion chromatography (Table 2 and Fig. 2). It is worth noting that the *E. coli* expression strain described here has proved to be useful for obtaining several other *P. torridus* enzymes in the native form, which were otherwise misfolded or not expressed at all (unpublished data).

AglA. The apparent size of the purified recombinant AglA enzyme estimated by SDS-PAGE (approximately 74 kDa) is in good agreement with the size calculated from the primary structure (75.4 kDa). The size of the native enzyme, determined by analytical gel permeation chromatography, was calculated to be 440 kDa, which suggests that AglA is active as a hexamer.

Using a 10-min assay, the purified recombinant α-glucosidase was found to be most active at 87°C when it was tested with *p*-nitrophenyl α-D-glucopyranoside in 50 mM acetate buffer at pH 5.0. Remarkably, this temperature is 27°C above the optimum growth temperature of *P. torridus* and more than 20°C above its maximum growth temperature. At 60°C the enzyme showed 23% of its maximal activity. Also, AglA retained considerable activity (81%) after preincubation of the enzyme for 120 min at 80°C. The kinetics of heat inactivation at temperatures between 70°C and 90°C appeared to be first

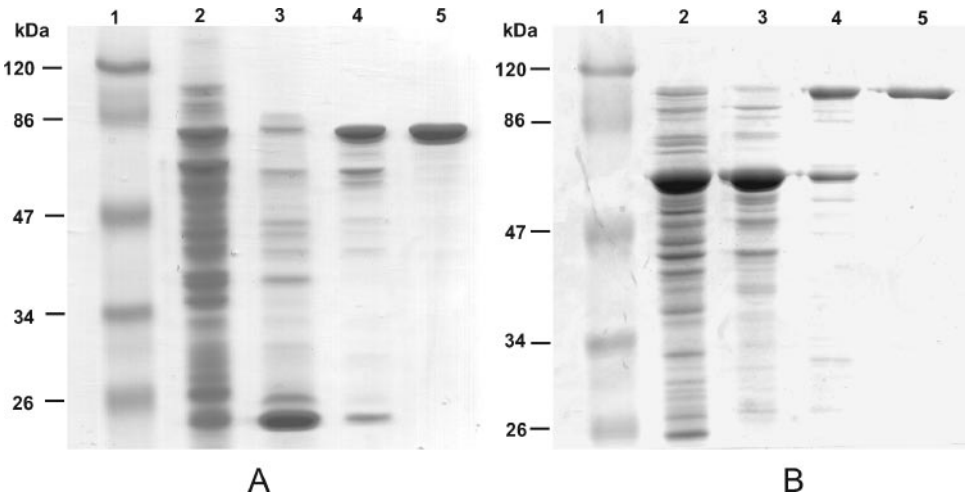

FIG. 2. SDS-PAGE analysis of the steps in the purification of recombinant *P. torridus* α-glucosidase (A) and α-mannosidase (B). (A) Lane 1, molecular weight marker; lane 2, *E. coli* BL21RS::p24-aglA cellular extract (8 μg); lane 3, heat-treated extract (5 μg); lane 4, AglA pooled fractions after anion-exchange chromatography (2 μg); lane 5, AglA pooled fractions after gel filtration chromatography (2 μg). (B) Lane 1, molecular weight marker; lane 2, *E. coli* BL21RS::p24-manA cellular extract (8 μg); lane 3, ManA pooled fractions after hydrophobic interaction chromatography (5 μg); lane 4, ManA pooled fractions after anion-exchange chromatography (3 μg); lane 5, ManA pooled fractions after gel filtration chromatography (0.7 μg).

TABLE 3. Characteristics of AglA and ManA

Enzyme	Substrate	Optimum pH	Optimum temp (°C)	K_m	V_{max}	k_{cat} (s^{-1})
AglA	*p*-Nitrophenyl-α-glucoside	5.0	87	0.94 ± 0.14	51.8 ± 1.57	65.1
	Maltose	5.0	87	3.7 ± 0.32	149.7 ± 3.9	188.1
ManA	*p*-Nitrophenyl-α-mannoside	5.2	70	0.49 ± 0.03	56.5 ± 3.1	105.1

order (data not shown). The enzyme displayed significant activity over a broad pH range, with maximum activity at pH 5.0. The optimum pH for AglA activity corresponds well to the reported intracellular pH of *Picrophilus* cells, pH 4.6 (35).

The substrate specificity of the enzyme was tested with a panel of oligosaccharides (maltose, isomaltose, maltotriose, maltotetraose, panose, trehalose, melibiose, sucrose, raffinose, turanose, melizitose, and α-, β- and γ-cyclodextrins) and polysaccharides (dextrin 10, amylose, starch, glycogen, and dextran), as well as with synthetic aryl glycosides (*p*-nitrophenyl-linked α- and β-glucopyranosides, α- and β-galactopyranosides, α- and β-xylopyranosides, and α-mannopyranoside). AglA showed the highest activity with maltose, and it hydrolyzed *p*-nitrophenyl α-D-glucopyranoside with a lower efficiency (Table 3). Strict specificity was observed both for the glycone residue of synthetic substrates (only glucose was accepted) and for the type of the glycosidic bond (only α-1,4 bonds were cleaved). The rate of maltooligosaccharide hydrolysis decreased with increasing number of maltose units in the substrate. Still, considerable activity was observed with maltotetraose (54% of the activity with maltose) or dextrin 10 (27%). In contrast to the closely related homolog from *S. solfataricus* or α-glucosidases of mammalian origin, AglA was unable to release glucose from polymeric substrates, like glycogen (24). Thin-layer chromatography analyses of the reaction products of AglA showed that only glucose was formed when maltooligosaccharides with different chain lengths were used as substrates and that no transferase activity was evident (Fig. 3, A). This substrate utilization spectrum indicates that AglA is a typical maltase enzyme (EC 3.2.1.20).

ManA. The elution profile of the recombinant *P. torridus* α-mannosidase in gel permeation chromatography under native conditions suggested that the size of this enzyme is 220 kDa, which corresponds to a dimer consisting of 111.5-kDa subunits. A small fraction of ManA activity could also be detected at approximately 120 kDa, most probably reflecting single subunits.

The maximum activity of ManA was observed at 70°C and pH 5.2 when pNP-Man was used as the substrate. ManA displayed an unusual metal requirement for activity; Cd^{2+} at a concentration of 1 mM was found to be the most potent activator (12.5-fold activation compared to the apoenzyme), followed by Co^{2+} (8.3-fold activation at a concentration of 10 mM), Fe^{2+} (4.5-fold activation at a concentration of 10 mM), and Mn^{2+} (3.8-fold activation at a concentration of 10 mM). EDTA abolished this activation completely when it was supplied in equimolar amounts or in excess. Zn^{2+}, Ca^{2+}, Mg^{2+}, Ba^{2+}, K^{+}, and Li^{+} had no significant effect on ManA activity when they were added at a concentration of 1 mM or 10 mM in the assay, while Ag^{+}, Ni^{2+}, Cu^{2+}, and Fe^{3+} were strong inhibitors at these concentrations. In addition, the resistance of ManA to heat inactivation (at 80°C) was increased considerably by the presence of Co^{2+} in the incubation buffer, and this effect was also neutralized by EDTA (Fig. 4). An inactive apoenzyme was obtained by dialysis of the purified ManA against 50 mM acetate buffer (pH 5.6) containing 5 mM EDTA, followed by a second dialysis against the same buffer without EDTA. Cd^{2+}, Co^{2+}, and Fe^{2+} at a concentration of 5 mM were able to completely restore the activity of the EDTA-

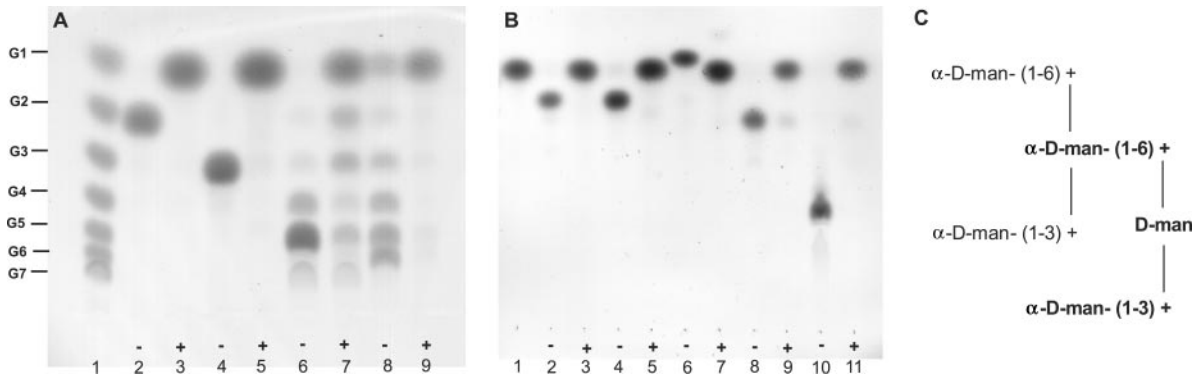

FIG. 3. Thin-layer chromatography analysis of the reaction products of *P. torridus* α-glucosidase (A) and α-mannosidase (B). (C) Schematic diagram of the structure of α3,α6-mannopentaose. The common core mannotriose structure found in N-glycans is indicated by boldface type. The reactions were carried out in 20 μl of 50 mM acetate buffer (pH 5.0) with 0.2% substrate and with (+) or without (−) 3.6 μg of purified AglA enzyme at 85°C (A) or with (+) or without (−) 0.3 μg of purified ManA at 65°C (B) for 4 h. (A) Lane 1, G1 to G7 maltooligosaccharide standards; lanes 2 and 3, maltose; lanes 4 and 5, maltotriose; lanes 6 and 7, maltopentaose; lanes 8 and 9, maltohexaose. (B) Lane 1, mannose; lanes 2 and 3, 1,2-α-mannobiose; lanes 4 and 5, 1,3-α-mannobiose; lanes 6 and 7, methyl-*O*-1,4-α-mannobiose; lanes 8 and 9, 1,6-α-mannobiose; lanes 10 and 11, α3,α6-mannopentaose.

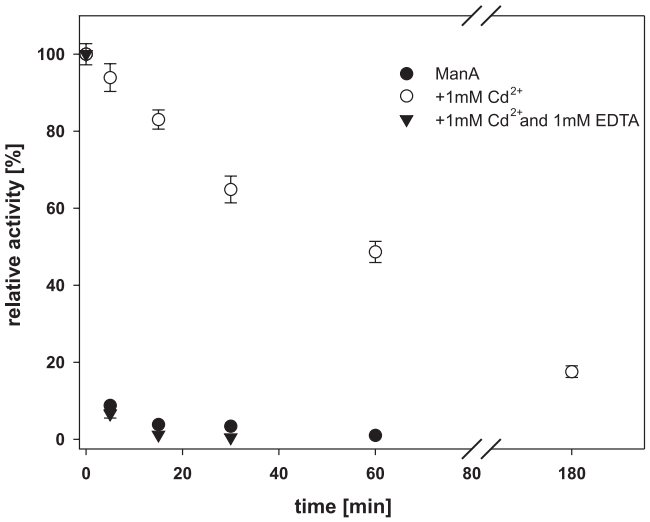

FIG. 4. Temperature inactivation kinetics of recombinant *P. torridus* α-mannosidase at 80°C. The purified enzyme (0.1 mg/ml) was incubated at 80°C in 50 mM acetate buffer (pH 5.0) with different additives, samples were withdrawn, and the residual activities were determined as described in Materials and Methods. Relative activity is expressed as the percentage of the activity without heat treatment.

treated enzyme, while incubation of the apoenzyme with Zn^{2+}, Ca^{2+}, Mg^{2+}, and Ba^{2+} did not lead to measurable restoration of activity.

The specificity of *P. torridus* α-mannosidase was examined with mannobiose substrates having all possible types of α-linkages (1→2, 1→3, 1→4, and 1→6), as well as with α3,α6-mannopentaose, which is the core structure of some triantennary N-linked carbohydrates in glycoproteins. TLC analysis of the reaction products after incubation of ManA with these substrates revealed that the enzyme has broad specificity and released mannose from all of the substrates (Fig. 3B and C). In addition, ManA was equally active with these mannobiose substrates when the released mannose was quantified, resulting in a specific activity of approximately 6.6 U/mg under optimal conditions. In order to examine the possible role of *P. torridus* α-mannosidase in the turnover of mannose-containing compatible solutes, the enzyme was incubated with 2-α-mannosyl-D-glycerate. No free mannose was detected after incubation of ManA for 12 h with this substrate either by TLC or by an enzymatic coupled assay.

Inhibition profile of ManA. Eukaryal α-mannosidases display different behaviors in the presence of the specific inhibitors 1-deoxymannojirimycin and swainsonine depending on their class affiliation. Class I enzymes are generally inhibited by 1-deoxymannojirimycin but not by swainsonine, while class II and III α-mannosidases have the opposite inhibition profile (6, 8, 29). As no archaeal representatives have been characterized previously, we examined the effects of these inhibitors on *P. torridus* α-mannosidase. Deoxymannojirimycin had no effect on ManA at concentrations up to 500 μM, while swainsonine showed competitive inhibition when pNP-Man was used as a substrate (Fig. 5A and B). In Fig. 5C the results for inhibition by swainsonine at two different substrate concentrations are presented as a Dixon plot, which revealed a K_i of 1.22 μM.

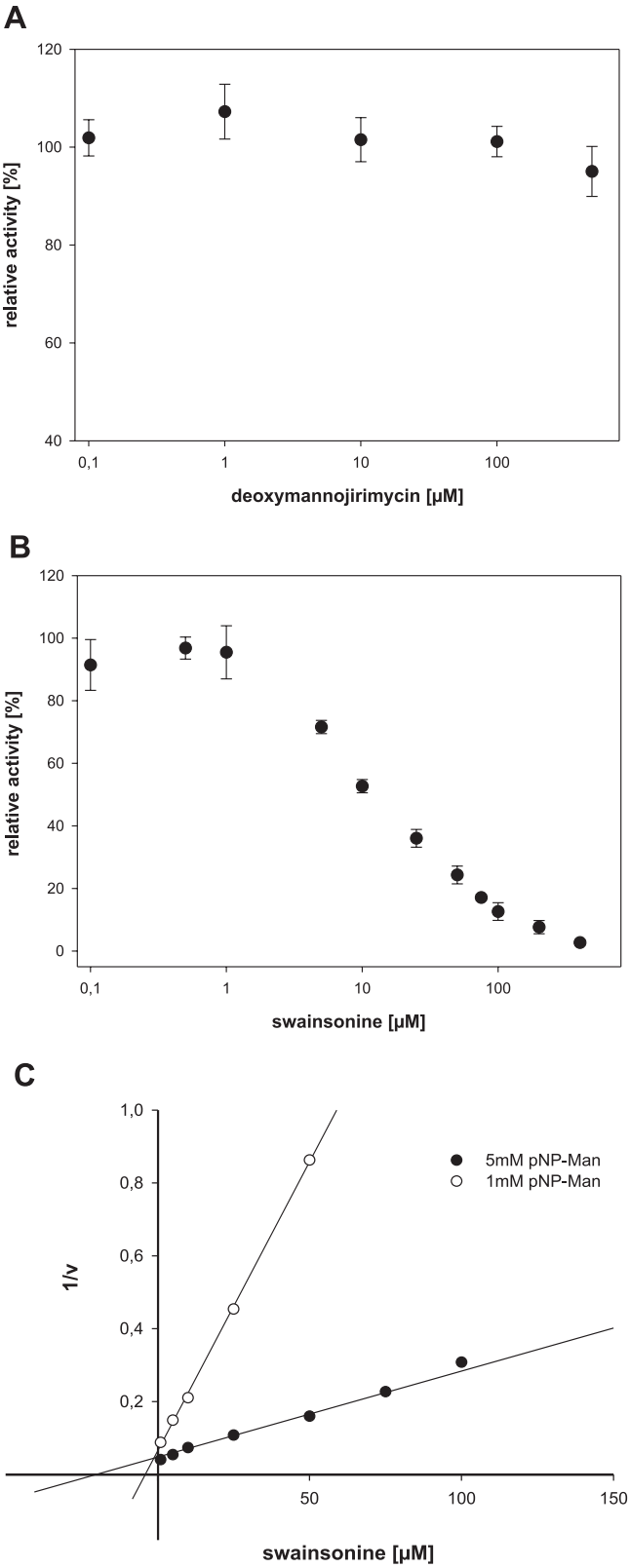

FIG. 5. Inhibition profile of *P. torridus* α-mannosidase. The enzyme (0.26 μg) was incubated for 15 min at 70°C in 50 mM acetate buffer (pH 5.0) with pNP-Man and different concentrations of the inhibitors deoxymannojirimycin (A) and swainsonine (B). (C) Dixon plot of the inhibition by swainsonine at two different substrate concentrations, resulting in a K_i of 1.22 μM.

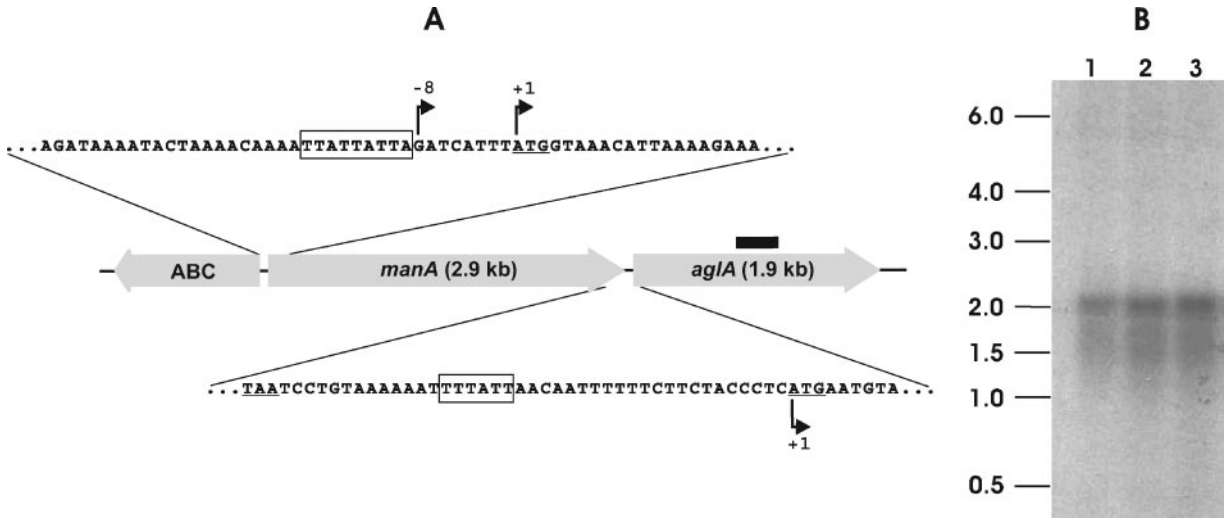

FIG. 6. (A) Genome region containing the *manA* and *aglA* genes (gray arrows). Start and stop codons are underlined, putative TATA box regions are enclosed in boxes, and the transcription start sites identified are indicated by bent arrows. (B) Northern blot analysis of the *aglA* gene. Lane 1 contained 2.5 μg total *P. torridus* RNA, and lanes 2 and 3 contained 5 μg total RNA isolated by two different methods (see Materials and Methods). The radioactive probe used for hybridization is indicated by a solid bar in panel A.

Genetic organization and transcription analysis of *P. torridus manA* and *aglA* genes. The *manA* and *aglA* genes are situated colinearly in the *P. torridus* genome and are separated by a 42-bp intergenic region. This functional cluster was found only in *P. torridus*; it was found in none of the organisms that possess orthologs of one of the two ORFs. Sequence analysis of the upstream gene regions revealed the presence of a nearly canonical TATA box sequence at position −28 relative to the start codon of the *aglA* gene and an adenine-rich region at positions −35 to −30, corresponding to an archaeal BRE element, while at −17 bp upstream of the *manA* gene a TA-rich sequence with only limited similarity to a TATA box was detected. Also, a poly(T) region was present 25 bp after the *manA* stop codon, possibly representing a termination signal. This finding pointed to the possibility that despite the colinear organization and the presumed physiological relatedness of the two genes, they might be transcribed separately. Therefore, we investigated whether the *manA* and *aglA* genes are cotranscribed. Initial RT-PCR experiments suggested that the two genes may be transcribed as a single message (not shown). However, further transcript analysis by Northern blotting yielded an approximately 2.1-kb fragment when the *aglA* DNA sequence was used as a probe, and no signal pointing to cotranscription (expected size, ~5 kb) was observed (Fig. 6B). In addition, 5′ RLM-RACE experiments showed the presence of a primary *aglA* transcript and revealed the *aglA* and *manA* transcription start sites. Therefore, we concluded that the RT-PCR products spanning the *manA-aglA* intergenic region that were obtained initially were most probably due to RNA polymerase readthrough (inefficient termination at end of the upstream gene). The *aglA* transcription start was mapped by 5′ RLM-RACE at the adenine of the start codon of the ORF (in plasmids from 10 individual clones analyzed), while two forms of the *manA* transcript were detected, starting at a guanine at position −8 (in 4 of 10 plasmids analyzed) and at an adenine at position 1 (in 6 of 10 plasmids analyzed) (Fig. 6A). Thus, both genes appeared to produce leaderless transcripts (transcripts lacking a 5′ untranslated region [5′-UTR]). The possibility that the *manA* and *aglA* genes are cotranscribed and processed further (cleaved) to generate two messages can be excluded because the 5′ RLM-RACE procedure distinguishes between primary (genuine) and processed transcripts based on their 5′ phosphorylation states (2). It has to be mentioned that in this case, transcript analysis by 5′ RLM-RACE is more informative than primer extension or S1 nuclease mapping, with which such discrimination cannot be made. The results from Northern hybridization and 5′ RLM-RACE indicate that the *aglA* gene is transcribed separately from its upstream neighbor *manA* and lacks a 5′-UTR.

Furthermore, we performed absolute *aglA* and *manA* mRNA quantification analyses with total *P. torridus* RNA preparations by using quantitative RT-PCR. The results obtained for the *manA* transcripts (4.14×10^6 molecules/reaction mixture; interassay coefficient of variation, 3.2%) and for the *aglA* transcripts (6.63×10^7 molecules/reaction mixture; interassay coefficient of variation, 2.7%) show that there was an approximately 16-fold excess of *aglA* mRNA compared to the amount of *manA* mRNA. These data are also consistent with independent transcription initiation of the downstream *aglA* gene, since normally internal operon genes are transcribed less efficiently.

DISCUSSION

Phylogenetic and biochemical analysis. Phylogenetic analysis clustered *P. torridus* α-glucosidase together with sequences of members of the distantly related crenarchaeal genus *Sulfolobus* rather than with the polypeptides from the closely related genus *Thermoplasma* (Fig. 1). It has been hypothesized that extensive lateral gene transfer occurred between these two lineages (10, 25). Therefore, it was not surprising to observe that AglA displayed properties similar to those of the previ-

ously characterized *S. solfataricus* homolog MalS (23, 24). The remarkable stability of the enzyme against thermoinactivation and its "optimum temperature" (27°C above the optimal growth temperature of *P. torridus*, measured under the standard assay conditions) are in agreement with the phylogenetic allocation of the AglA sequence and support the hypothesis that there was a gene transfer event. In this respect it would be interesting to examine the currently uncharacterized AglA homologs found in other euryarchaea, like *T. acidophilum* and *T. volcanium* (accession numbers CAC11443 and BAB60467, respectively). Most probably, the *P. torridus* α-glucosidase plays an important role in the pathway for utilization of α-glucans like starch (30) and of maltooligosaccharides. No ortholog of a maltodextrin phosphorylase was found in the *P. torridus* genome, suggesting that maltose (maltodextrin) hydrolysis is the only means of linking these substrates to glycolysis.

To our knowledge, the *P. torridus* α-mannosidase enzyme described here is the first characterized archaeal member of GHF 38. Together, the observed broad substrate spectrum, the lack of a signal peptide sequence, the inhibition profile, and the unusual metal requirements of ManA suggest that it is a cytosolic enzyme belonging to the class III α-mannosidases. A role of *P. torridus* α-mannosidase in the utilization and/or turnover of compatible solutes like 2-α-D-mannosyl-glycerate can be ruled out, as ManA was inactive with this compound. In agreement, the genome of *P. torridus* does not contain genes for key enzymes necessary for 2-α-D-mannosyl-glycerate synthesis (e.g., mannosyl-3-phosphoglycerate synthase and mannosyl-3-phosphoglycerate phosphatase). Another possible role for ManA is a contribution to the utilization of exogenous glycoproteins and/or to the turnover of the organism's own glycoproteins, specifically in metabolizing the glycone moiety, which was shown to be a substrate for ManA. Indeed, in the closely related organism *T. acidophilum*, it has been reported that there are glycoproteins with high mannose contents (37), and a functional glycosylation system (dolichyl-phosphomannose synthase) has been described (38). Protein glycosylation in *P. torridus* has not been studied biochemically. Analysis of the *P. torridus* genome revealed at least two possible routes for metabolizing the released mannose, through a mannose dehydrogenase and mannonate dehydratase (PTO0149), yielding 2-keto-3-deoxygluconate (KDG), which is part of the Entner-Doudoroff pathway, or via a mannose-6-phosphate isomerase (PTO0939), yielding fructose-6-phosphate, which can be channeled into glycolysis.

Molecular analysis. Transcription initiation in members of the *Archaea* has been extensively studied (32). However, most of the data comes from experiments with representatives of the halophilic *Archaea* (*Haloferax*), methanogens (*Methanococcus*), and *Crenarchaeota* (*Sulfolobus*). In contrast, information about the mode of transcription initiation and the regulatory elements that govern it in species of the *Thermoplasma* group is very limited.

The experiments aimed at elucidating the mode of transcription of the *P. torridus* α-mannosidase and α-glucosidase genes credibly showed that these genes have separate transcription initiation sites despite the colinear orientation and the small 42-bp intergenic region. A cotranscript could not be detected by Northern blot analysis or 5′ RLM-RACE. A PCR product spanning the intergenic region which was found in RT-PCR experiments was most probably due to inefficient termination at the end of the upstream gene (*manA*).

The presence of leaderless mRNA has been described in very diverse taxa (*Bacteria*, *Archaea*, and *Eukarya*), and there is experimental evidence that such mRNA is capable of initiating translation (reference 36 and references therein). In the *Archaea*, such an unusual transcription start site has been computationally predicted for *S. solfataricus* (34) and has been experimentally shown for 10 genes in *Pyrobaculum aerophilum* (31); both of these organisms are members of the *Crenarchaeota*. Also experimentally, transcription has been shown to initiate at the adenine in the first codon of the *S. solfataricus lacS* (β-glycosidase) gene (14). Notably, the *P. torridus aglA* gene was shown to produce a leaderless transcript, and the *manA* gene was found to have two distinct transcription initiation sites, one of which also produced an mRNA lacking a 5′-UTR. The 5′ RLM-RACE method used in the present study did not allow quantification of the alternative transcripts and did not allow us to address whether growth on different media has an effect on the *manA* transcription start site selection. However, the results of the experiments provide additional and independent proof for the presence of primary (5′-triphosphate-containing), leaderless mRNA in archaea, as the currently available evidence was derived from primer extension and S1 nuclease mapping assays.

Currently, the mechanism for translation of leaderless RNA is not completely clear. One hypothesis proposes the existence of downstream sequence elements that interact with rRNA (16, 33). Another possibility, which does not necessarily exclude the first possibility, is participation of *trans*-acting elements like initiation factor 2 (13).

Whole-genome computational analyses have suggested that in *Crenarchaeota* two distinct gene groups can be defined based on conserved sequences in their upstream regions. One group has well-defined Shine-Dalgarno (SD) sequences and consists of internal operon genes, whereas the second group lacks detectable SD sequences and includes single or operon-initiating genes (34). Since SD sequences are readily detected in several of the sequenced euryarchaeal genomes (19), it remains to be determined whether the leaderless transcription reported here is a general phenomenon or an exception in *P. torridus* and in representatives of the closely related genus *Thermoplasma*.

ACKNOWLEDGMENTS

We thank E. Galinski (Bonn, Germany) for providing 2-α-mannosyl-D-glycerate and Mechthild Bömeke for excellent technical support.

REFERENCES

1. **Bendtsen, J. D., H. Nielsen, G. von Heijne, and S. Brunak.** 2004. Improved prediction of signal peptides: SignalP 3.0. J. Mol. Biol. **340:**783–795.
2. **Bensing, B. A., B. J. Meyer, and G. M. Dunny.** 1996. Sensitive detection of bacterial transcription initiation sites and differentiation from RNA processing sites in the pheromone-induced plasmid transfer system of *Enterococcus faecalis*. Proc. Natl. Acad. Sci. USA **93:**7794–7799.
3. **Costantino, H. R., S. H. Brown, and R. M. Kelly.** 1990. Purification and characterization of an alpha-glucosidase from a hyperthermophilic archaebacterium, *Pyrococcus furiosus*, exhibiting a temperature optimum of 105 to 115°C. J. Bacteriol. **172:**3654–3660.
4. **Coutinho, P. M., and B. Henrissat.** 1999. Carbohydrate-active enzymes: an integrated database approach, p. 3–12. *In* H. J. Gilbert, G. Davies, B. Henrissat, and B. Svensson (ed.), Recent advances in carbohydrate bioengineering. The Royal Society of Chemistry, Cambridge, United Kingdom.
5. **Daniel, P. F., B. Winchester, and C. D. Warren.** 1994. Mammalian alpha-mannosidases—multiple forms but a common purpose? Glycobiology **4:**551–566.

6. **Dorling, P. R., C. R. Huxtable, and S. M. Colegate.** 1980. Inhibition of lysosomal alpha-mannosidase by swainsonine, an indolizidine alkaloid isolated from *Swainsona canescens*. Biochem. J. **191:**649–651.
7. **Eades, C. J., A. M. Gilbert, C. D. Goodman, and W. E. Hintz.** 1998. Identification and analysis of a class 2 alpha-mannosidase from *Aspergillus nidulans*. Glycobiology **8:**17–33.
8. **Elbein, A. D.** 1991. Glycosidase inhibitors: inhibitors of N-linked oligosaccharide processing. FASEB J. **5:**3055–3063.
9. **Ernst, H. A., L. Lo Leggio, M. Willemoes, G. Leonard, P. Blum, and S. Larsen.** 2006. Structure of the *Sulfolobus solfataricus* alpha-glucosidase: implications for domain conservation and substrate recognition in GH31. J. Mol. Biol. **358:**1106–1124.
10. **Etchison, J. R., and H. H. Freeze.** 1997. Enzymatic assay of D-mannose in serum. Clin. Chem. **43:**533–538.
11. **Fütterer, O., A. Angelov, H. Liesegang, G. Gottschalk, C. Schleper, B. Schepers, C. Dock, G. Antranikian, and W. Liebl.** 2004. Genome sequence of *Picrophilus torridus* and its implications for life around pH 0. Proc. Natl. Acad. Sci. USA **101:**9091–9096.
12. **Gonzalez, D. S., and I. K. Jordan.** 2000. The alpha-mannosidases: phylogeny and adaptive diversification. Mol. Biol. Evol. **17:**292–300.
13. **Grill, S., C. O. Gualerzi, P. Londei, and U. Blasi.** 2000. Selective stimulation of translation of leaderless mRNA by initiation factor 2: evolutionary implications for translation. EMBO J. **19:**4101–4110.
14. **Hoang, V., E. Bini, V. Dixit, M. Drozda, and P. Blum.** 2004. The role of cis-acting sequences governing catabolite repression control of *lacS* expression in the archaeon *Sulfolobus solfataricus*. Genetics **167:**1563–1572.
15. **Kumar, S., K. Tamura, and M. Nei.** 1994. MEGA: Molecular Evolutionary Genetics Analysis software for microcomputers. Comput. Applic. Biosci. **10:**189–191.
16. **Martin-Farmer, J., and G. R. Janssen.** 1999. A downstream CA repeat sequence increases translation from leadered and unleadered mRNA in *Escherichia coli*. Mol. Microbiol. **31:**1025–1038.
17. **Maruyama, Y., T. Nakajima, and E. Ichishima.** 1994. A 1,2-alpha-D-mannosidase from a *Bacillus* sp.: purification, characterization, and mode of action. Carbohydr. Res. **251:**89–98.
18. **Nakajima, M., H. Imamura, H. Shoun, and T. Wakagi.** 2003. Unique metal dependency of cytosolic alpha-mannosidase from *Thermotoga maritima*, a hyperthermophilic bacterium. Arch. Biochem. Biophys. **415:**87–93.
19. **Osada, Y., R. Saito, and M. Tomita.** 1999. Analysis of base-pairing potentials between 16S rRNA and 5′ UTR for translation initiation in various prokaryotes. Bioinformatics **15:**578–581.
20. **Pfaffl, M. W., and M. Hageleit.** 2001. Validities of mRNA quantification using recombinant RNA and recombinant DNA external calibration curves in real-time RT-PCR. Biotechnol. Lett. **23:**275–282.
21. **Piller, K., R. M. Daniel, and H. H. Petach.** 1996. Properties and stabilization of an extracellular alpha-glucosidase from the extremely thermophilic archaebacteria *Thermococcus* strain AN1: enzyme activity at 130°C. Biochim. Biophys. Acta **1292:**197–205.
22. **Rivera-Marrero, C. A., J. D. Ritzenthaler, J. Roman, and K. W. Moremen.** 2001. Molecular cloning and expression of an alpha-mannosidase gene in *Mycobacterium tuberculosis*. Microb. Pathog. **30:**9–18.
23. **Rolfsmeier, M., and P. Blum.** 1995. Purification and characterization of a maltase from the extremely thermophilic crenarchaeote *Sulfolobus solfataricus*. J. Bacteriol. **177:**482–485.
24. **Rolfsmeier, M., C. Haseltine, E. Bini, A. Clark, and P. Blum.** 1998. Molecular characterization of the alpha-glucosidase gene (*malA*) from the hyperthermophilic archaeon *Sulfolobus solfataricus*. J. Bacteriol. **180:**1287–1295.
25. **Ruepp, A., W. Graml, M. L. Santos-Martinez, K. K. Koretke, C. Volker, H. W. Mewes, D. Frishman, S. Stocker, A. N. Lupas, and W. Baumeister.** 2000. The genome sequence of the thermoacidophilic scavenger *Thermoplasma acidophilum*. Nature **407:**508–513.
26. **Sambrook, J., E. F. Fritsch, and T. Maniatis.** 1989. Molecular cloning: a laboratory manual, 2nd ed. Cold Spring Harbor Laboratory, Cold Spring Harbor, N.Y.
27. **Sampaio, M. M., F. Chevance, R. Dippel, T. Eppler, A. Schlegel, W. Boos, Y. J. Lu, and C. O. Rock.** 2004. Phosphotransferase-mediated transport of the osmolyte 2-O-alpha-mannosyl-D-glycerate in *Escherichia coli* occurs by the product of the *mngA* (*hrsA*) gene and is regulated by the *mngR* (*farR*) gene product acting as repressor. J. Biol. Chem. **279:**5537–5548.
28. **Schleper, C., G. Puehler, I. Holz, A. Gambacorta, D. Janekovic, U. Santarius, H. P. Klenk, and W. Zillig.** 1995. *Picrophilus* gen. nov., fam. nov.: a novel aerobic, heterotrophic, thermoacidophilic genus and family comprising archaea capable of growth around pH 0. J. Bacteriol. **177:**7050–7059.
29. **Schutzbach, J. S., and W. T. Forsee.** 1990. Calcium ion activation of rabbit liver alpha 1,2-mannosidase. J. Biol. Chem. **265:**2546–2549.
30. **Serour, E., and G. Antranikian.** 2002. Novel thermoactive glucoamylases from the thermoacidophilic Archaea *Thermoplasma acidophilum*, *Picrophilus torridus* and *Picrophilus oshimae*. Antonie Leeuwenhoek **81:**73–83.
31. **Slupska, M. M., A. G. King, S. Fitz-Gibbon, J. Besemer, M. Borodovsky, and J. H. Miller.** 2001. Leaderless transcripts of the crenarchaeal hyperthermophile *Pyrobaculum aerophilum*. J. Mol. Biol. **309:**347–360.
32. **Soppa, J.** 1999. Transcription initiation in Archaea: facts, factors and future aspects. Mol. Microbiol. **31:**1295–1305.
33. **Sprengart, M. L., E. Fuchs, and A. G. Porter.** 1996. The downstream box: an efficient and independent translation initiation signal in *Escherichia coli*. EMBO J. **15:**665–674.
34. **Tolstrup, N., C. W. Sensen, R. A. Garrett, and I. G. Clausen.** 2000. Two different and highly organized mechanisms of translation initiation in the archaeon *Sulfolobus solfataricus*. Extremophiles **4:**175–179.
35. **van de Vossenberg, J. L., A. J. Driessen, W. Zillig, and W. N. Konings.** 1998. Bioenergetics and cytoplasmic membrane stability of the extremely acidophilic, thermophilic archaeon *Picrophilus oshimae*. Extremophiles **2:**67–74.
36. **Wu, C. J., and G. R. Janssen.** 1996. Translation of *vph* mRNA in S*treptomyces lividans* and *Escherichia coli* after removal of the 5′ untranslated leader. Mol. Microbiol. **22:**339–355.
37. **Yang, L. L., and A. Haug.** 1979. Purification and partial characterization of a prokaryotic glycoprotein from the plasma membrane of *Thermoplasma acidophilum*. Biochim. Biophys. Acta **556:**265–277.
38. **Zhu, B. C., and R. A. Laine.** 1996. Dolichyl-phosphomannose synthase from the archae *Thermoplasma acidophilum*. Glycobiology **6:**811–816.
39. **Zychlinsky, E., and A. Matin.** 1983. Cytoplasmic pH homeostasis in an acidophilic bacterium, *Thiobacillus acidophilus*. J. Bacteriol. **156:**1352–1355.